DUJASE Vol. 6 (1) 58-65, 2021 (January)

Fabrication and Characterization of the CZTS (Cu_2ZnSnS_4) Thin Film Absorption Layer Using Easy and Low Cost Sol-gel Dip-coating Technique

M Rahman[1], N Islam[1*], Rummana Matin[2] and M S Bashar[2]

[1] *Department of Physics, University of Dhaka, Bangladesh*
[2] *IFRD, BCSIR, Dhaka, Bangladesh*

[*] *E-mail : naimul.islam@gmail.com*

Received on 24.03.21, Accepted for publication on 14.6.21

ABSTRACT

Cu_2ZnSnS_4 (CZTS) thin films were developed through sol-gel dip-coating method. These films were annealed in vacuum at 550°C and further characterized by UV–vis spectroscopy, X-ray diffraction (XRD), scanning electron microscopy (SEM), and energy dispersive X-ray spectroscopy (EDS) procedures. The CZTS films exhibited tremendous optical absorption (2×10^4 cm^{-1}) and demonstrated band gap energy of 1.58 eV. X-ray diffraction analysis revealed the formation of kesterite structure of CZTS films. Scanning electron micrograph displayed the formation of densely packed, compact and large grained CZTS films. The thin film indicated irregular dissemination of agglomerated particles with well-defined boundaries. The energy dispersive X-ray spectroscopy study gave the stoichiometric ratio as Cu: Zn: Sn: S=1.9:1.35:1:5.2.

Keywords: Thin film, Sol-gel, Buffer Layer, Solar Cells, CZTS (Cu_2ZnSnS_4), XRD, SEM, EDS

1. Introduction

Polycrystalline thin film solar cells, such as cadmium telluride (CdTe), copper indium selenide (CIS), and copper indium gallium selenide (CIGS) have drawn abundant attention in the past few decades [1-3]. While CIGS and CdTe solar cells have high power conversion efficiencies (PCE) (>11% in module production and 20% in laboratory), they have constraints due to the shortage of In, Ga and Te, and the ecological effects related with the deadliness of Cd and Se [4, 5]. To get rid of these problems, the I_2–II–IV–VI_4 quaternary compounds, for instance Cu_2ZnSnS_4 (CZTS) and $Cu_2ZnSnSe_4$ (CZTSe), have drawn substantial attractions and been viewed as one of the most encouraging 'next generation' photovoltaic materials because of their near-optimum direct band gap energy (1.4∼1.6eV), large absorption coefficient ($>10^4 cm^{-1}$) and theoretical high power conversion efficiency (~ 32.2%)[6, 7]. Therefore, CZTS/CZTSe can be accepted as an alternative to $Cu(In,Ga)Se_2$ (CIGS).Meanwhile, their elements, Zn and Sn are harmless and earth-abundant (Cu: 50ppm, Zn: 75ppm, Sn: 2.2ppm, S: 260ppm) as to the elements of CIGS[8], hence less costly than In and Ga. Therefore, to promote solar cells without the ecological pollutants, CZTS is considered as a probable successor for the absorber layer of the next generation thin film solar cells and several researchers have shown considerable success in this field.

Several deposition techniques, like pulsed laser deposition [9], thermal evaporation [10], chemical vapour deposition [11] and sputtering deposition [12], have been adopted by the researchers for fabrication of CZTS thin films. However, thin film deposition technique still requiressomewhat precise processing circumstances (e.g., high temperature, high vacuum or expensive raw chemicals) to achievejustifiable effectiveness which eventually increase the cost of fabrication. Therefore, several research groups have investigated to develop CZTS films atatmospheric conditions [13-15] to reduce the cost.To date, the best CZTS thin-film solar cells have been produced employing a hydrazine-based non-vacuum means, and these gave a PCE of 12.6% [16, 17]. Nonetheless, the PCE of CZTS is yetunder the PCE of CIGS thin-film solar cells (η>21%)[5, 18]. Moreover, hydrazine is extremely poisonous and volatile compound that needs utmost care for storage[19]. Thus, a robust, scalable, and somewhat safe solution-based technique for the fabrication of CZTS thin films that results in high efficiency is preferable needed.

In addition, there are various other factors that can curtail the efficacy of CZTS thin-film solar cells. Though CZTS thin film solar cell has higher band gap than that of other thin film solar cell, it gives low open circuit voltage (VOC) [20]. The CZTS solar cells has low minority carrier lifetime of about several nanoseconds [21]. However, CZTS solar cell requires high minority carrier life time. Moreover, it is challenging to develop a perfect CZTS phase from Cu, Zn, Sn, and S due to the formation of abundant auxiliary phases all along the fabrication[22].

Until now, the appropriate structure of CZTS thin-film solar cells has not been distinctly specified. The kesterite structured CZTS thin film is an obscureelement and vulnerable to deformity. Moreover, deviation of the environments of the precursor have a decent consequence on the phase composition of keserite and afterwards on the efficacy of solar cells. Usually, Cu-poor and Zn-rich compositions of CZTS solar cells have been reported to have high efficiency [17,21,23-27]. Nonetheless, Hsu et al. reported that Cu-rich and Zn-rich solar cells with a close stoichiometric content can have a conversion efficiency more than 9% [28].

The CZTS configuration influence the evolution of secondary phases. For instance, a Cu-rich configuration quickly develops a Cu_2S secondary phase whereas Sn-rich and Zn-rich configurations subsequently endorse the evolution of SnS and ZnS secondary phases [27, 29]. So, a single pure CZTS phase is necessary to obtain which do not

have secondary phases. Fairbrother et al. and Platzer-Björkman et al. suggested that adjustment of the occupancy of Zn manipulate the behaviour of CZTS thin-film solar cells. A Zn-rich configuration quickly develop ZnS secondary phases that deteriorate functioning of the device [30, 31]. Guan et al. observed that ZnS contaminations restrict the build-up of voids in the CZTS nano-crystals, and the region of these ZnS pollutants governs the achievement of the CZTS solar cells. The formation of ZnS on the top of the CZTS has negative influence on the functioning of the cells, whereas the consequence of ZnS on the rear of the CZTS are insignificant. The ZnS impurities are situated all over the whole layer or situated atthe rear connection of the CZTS, and the excessive resistance of ZnS restricts the shipment of photo-generated carriers within the CZTS solar cells [32]. Conversely, Zn-rich circumstances are favourable to bettering the functioning of CZTS devices as a result of boosting of the p-type conductivity and curtailing the formation of Cu_2SnS_3(CTS) secondary phases.

Herein, we have investigated the sol-gel approach to develop CZTS thin films absorption layer applying mono-ethanolamine as solvent and 2- methoxyethanol as stabilizer in the precursor. The solvent and stabilizer portrayed a powerful character in the system of preparing stable CZTS sol-gel precursor and manufacturing superior-quality CZTS films. Later, the structural, optical and electrical properties of the prepared thin films were investigated.

2. Material and methods

First, the CZTS thin films were synthesised from the precursor solutions and later the films were characterized.

2.1. Synthesis of the CZTS thin films

For deposition of the CZTS thin films we have used the easy and low cost sol-gel method. Large area thin films of different shapes can be prepared with this method without vacuum conditions. The composition of prepared films and its microstructure can be effectively controlled by this method.

First, the glass substrates were wiped carefully with a tissue paper soaked with methanol and deionized water respectively. After that, the glass slide was submerged in methanol for few minutes and followed by an ultrasonic bath for 10 minutes. Similarly, the glass slide was submerged in acetone and DI water respectively for few minutes followed by an ultrasonic bath for 10 minutes in both cases.

2.1.1 Preparation of the precursor solution

Next, precursor mixture was developed by mixing the solid and powder-formed Copper (II) Acetate Monohydrate ($Cu(CH_3COO)_2.H_2O$), Zinc Acetate Dihydrate ($Zn(CH_3COO)_2.2H_2O$), Tin (II) Chloride Dihydrate ($SnCl_2.2H_2O$) and Thiourea (CH_4N_2S) at room temperature. Next, the precursor mixture was dissolved in 2-methoxyethanol ($CH_3OCH_2CH_2OH$) and mono-ethanolamine ($(HOCH_2CH_2)NH_2$). The 2-methoxyethanol and mono-ethanolamine liquid acted as solvent and stabilizer for the precursor solution. All these chemicals were quite good and 95-100% pure. The molar concentration of chemicals used for the preparation of precursor solution was taken as 1.8, 1.2, 1 and 8M for Copper, Zinc, Tin, and Thiourea subsequently [33]. The precursor solution was continuously stirred with a stick for 5 minutes. Next, the solution was taken into a 200mL beaker, and placing the beaker on a hotplate the solution was stirred by a magnetic stirrer for homogenous and continuous mixing of the chemicals (Fig. **1**(a)). The solution was stirred until temperature reached to 70°C[34]. Then, at constant temperature 70°C the solution was further stirred for 30 minutes [34].

2.1.2 Deposition of the CZTS thin films

The CZTS thin films were deposited on glass substrates. Each glass substrate was dipped for 3 minutes into the sol-gel precursor (Fig. **1**-(b)). The glass slides were dipped into and picked up at three different dipping speeds - 100, 75, and $50ms^{-1}$. Three samples were prepared and labelled as sample 1, 2 and 3 respectively depending on the dipping speed.

The deposited glass slides were put into an oven for drying after raising the starting temperature of the oven to 150°C. Then, the temperature was raised to 250°C, and all the slides were kept in the oven for 30 minutes to remove the solvent and constituent elements from the CZTS thin films [34, 35]. The dried CZTS thin films were sulfurized in an annealing chamber (Fig. **1**-(c)) at 550°C, and then cooled down to the ambient temperature and left for a day to be stable.

2.2. Characterization techniques

2.2.1 Thickness measurements

The thickness "d" of a film was measured by using fully computerized BRUKER Dektak XT™ stylus profiler with unlimited repeatability of 4A° and very high scanning speed. The Dektak XT ran automated multi-site measurement routines to verify the precise measurement of thickness of films across the wafer surface down to nano-meter scale.

2.2.2 Optical characteristics measurements

The optical characteristics were measured using the UH4150, Hitachi, UV-vis spectrophotometer (Japan). The sample-coated glass substrates were placed vertically in the thin film holder of the spectrophotometer and then the samples were illuminated by a monochromatic beam of light. The relative transmittance, reflectance and absorbance of the deposited CZTS thin films were measured in wavelength range 300 to 700nm.

The absorption coefficient "α" of the CZTS thin films was computed from the measured relative absorbance data for different wavelengths corresponding to different photon energies at room temperature by using the Beer-Lambert law [26],

$$a = 2.303\ \frac{A}{d} \quad \text{..... (1)}$$

Where, $A = \log_{10}\left(\frac{I_0}{I}\right)$ is the absorbance, 'd' is the thickness of the film, 'I' is the intesity of light passing through the CZTS film and 'I_0' is the intesity of the incident light.

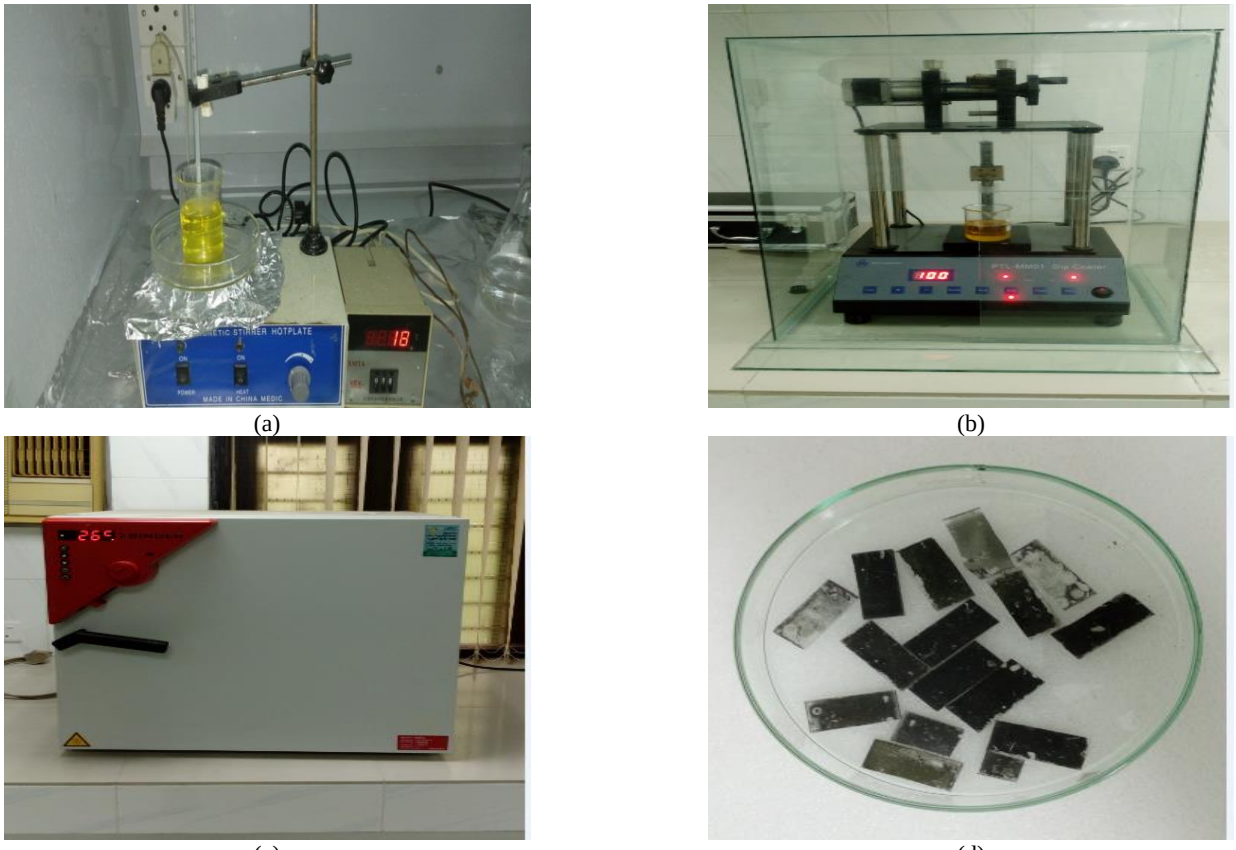

Fig. 1. The CZTS thin film synthesis process. (a) magnetic stirring process of the CZTS precursor solution using the 78-1 Magnetic Stirrer Hotplate (b) dip-coating of the slides using the PPL-MMD1 Dip Coater instrument (c) annealing of the CZTS glass slides using the DTPLCSP BINDER machine (d) the prepared CZTS thin films on glass substrate are shown on a petri dish.

2.2.3 Band Gap Measurements

The band gap energy "E_g" for different types of CZTS thin films was determined using the absorption coefficient values [35]. The absorption coefficient "α" is related to the photon energy "hν" by the following equation-

$$a = \frac{Ao(hv-Eg)^n}{hv} \quad \text{.....(2)}$$

Where 'A_o'is a constant related to the effective masses associated with bands and 'n'= 0.5 or 2 depending on direct or indirect bandgap materials [34]. Since CZTS is a direct band gap material, we have used the value of n equal to 0.5. So, simplifying the equation 2, we get

$$a = \frac{Ao(hv-Eg)^{0.5}}{hv} \quad \text{.....(3)}$$

$$(\alpha hv)^2 = A_o^2 (hv - E_g) \quad \text{.....(4)}$$

The optical band gap energy of the CZTS thin films was estimated using equation 4. The $(\alpha hv)^2$ values were plotted against photon energy (hν), which is known as the Tauc plot. The value of band gap energy is obtained by extrapolating the linear region of the Tauc plot to the intercept in the photon energy axis.

2.2.4 Structural Analysis

The X-ray diffraction method was used to investigate the structural properties of the CZTS films. The diffraction pattern was recorded using the GBC Matrix SSD XRD system. The Cu-Kα radiation was used to get the possible fundamental diffraction peaks from the sample. The machine was operated at 35.5kV and 28.5mA current. The room temperature was kept at 18°C and the scanning angle was fixed to the range $20^o \leq 2\theta \leq 70^o$ [36].

The lattice parameter for each sample was calculated by using the following formula,

$$\frac{1}{d^2} = \frac{h^2+k^2}{a^2} + \frac{l^2}{c^2} \quad \text{.....(5)}$$

Where h, k, and l are the miller indices of the crystal planes, a and c are lattice parameters which are constant for the specific thin film and d is the observed spacing given by,

$$d = \frac{\lambda}{2\sin\theta} \quad \text{.....(6)}$$

To get the value of d, the value of λ (= 0.15406 nm) and θ (observed from the XRD graph in degree) were put in equation (6). After putting the value of d in equation (5), 6 different equations were obtained. For determining the lattice parameters a & c, the miller indices h, k and l values ((112), (103), (220) and (312)) were used in these 6 equations and then solving these 6 equations, the expected values of lattice parameters a & c were obtained.

It is roughly possible to determine the particle size of the CZTS crystal from the full width at half maximum

(FWHM) of the diffraction peak at a particular plane (hkl) using the Debye-Scherrer formula[37]:

$$D = \frac{0.94\,\lambda}{\beta\,Cos(\theta)} \quad \text{.....(7)}$$

Where, 'D' is the mean particle size, λ is the wavelength of X-ray radiation (λ= 0.15406nm in our study), 'β' is the FWHM of the peak of (hkl) plane and 'θ' is the diffraction angle.

2.5 Surface morphology and compositional characterization

The SEM EVO 18 Research, Zeiss high performance scanning electron microscope was used to investigate the surface morphology and uniformity of the deposited CZTS thin films. The embedded energy dispersive X-ray analyser (EDAX) of the SEM was used for elemental analysis. The EDX analyser relies on the interaction of electron beam with the sample and the emission and detection of the characteristic X-rays from the compositional materials of the sample.

3. Results and Discussion

3.1 Thickness

Thickness is the most important parameter in the sense that, it modify the properties of thin film material owing to surface phenomena. To observe the change of film-thickness of the CZTS films with dip-coating speed, multiple samples from the same chemical were prepared with different dip-coating speeds. The film thickness did not change significantly with dipping speeds. The average thickness of the CZTS film was 1.24μm. Typically, absorption coefficient for the CZTS thin films is in the range of 10^4-$10^5$$cm^{-1}$ and for that a thicker absorber is required to absorb the solar spectrum efficiently and to cut down recombination (i.e. increase the minority carrier lifetimes) at the back contact [38, 39]. Todorov et al. suggested that absorber thickness greater than 2.5μm would increase the efficiency of CZTS thin film [40]. However, thicker absorber layers may also reduce efficiency due to the increased series resistance. Fig. **1**-(d) displays the photograph of consistent and compact CZTS thin films for 100, 75 and 50ms^{-1} dipping speed onto the clean glass substrate comprising area of 10cm^2, which validate the practicability of the sol-gel technique for sizable area CZTS film production.

3.2. Optical studies

The measured optical absorption, transmission and reflectance of the vacuum annealed CZTS thin films are shown in Fig. 2 with change of wavelengths.

These spectra affirmed that the CZTS thin films have very high absorbance (95.75, 98.3 and 95.9% respectively for the sample 1, 2, and 3) and very low transmittance (2.75-3.8%, 0.75-1.15% and 3.1-3.4% respectively for the sample 1, 2, and 3) and reflectance (0.65-0.85%, 0.4-0.5%, and 0.6-0.81% respectively for sample 1, 2 and 3) of light in the visible region. These indicated the applicability of these types of CZTS thin films as the absorber layer for solar cells. From the optical measurements, the absorption co-efficient of the prepared CZTS samples were calculated using equation 1. The obtained absorption coefficient was greater than the standard value ($10^4$$cm^{-1}$), however, similar finding was reported in earlier works [24, 26, 34, 36, 37, 41-46].

The optical band gap energy of the CZTS thin film was estimated utilising equation 4. Fig. 3 displays the changes of value $(\alpha h\nu)^2$ against hν, which shows a linear rise in the realm of higher energies, demonstrating a direct optical transition. Extrapolation of these curves to photon energy axis provides the average band gap energy of 1.85eV for the CZTS thin films. The CZTS thin films were compatible with band gaps notified for CZTS films by other authors [24, 26, 34, 36, 37, 41-49]. The band gap of the film is nearest to the optimum band gap (1.5eV) desired for a solar cell, demonstrating that CZTS is a promising material for thin film solar cell[50].

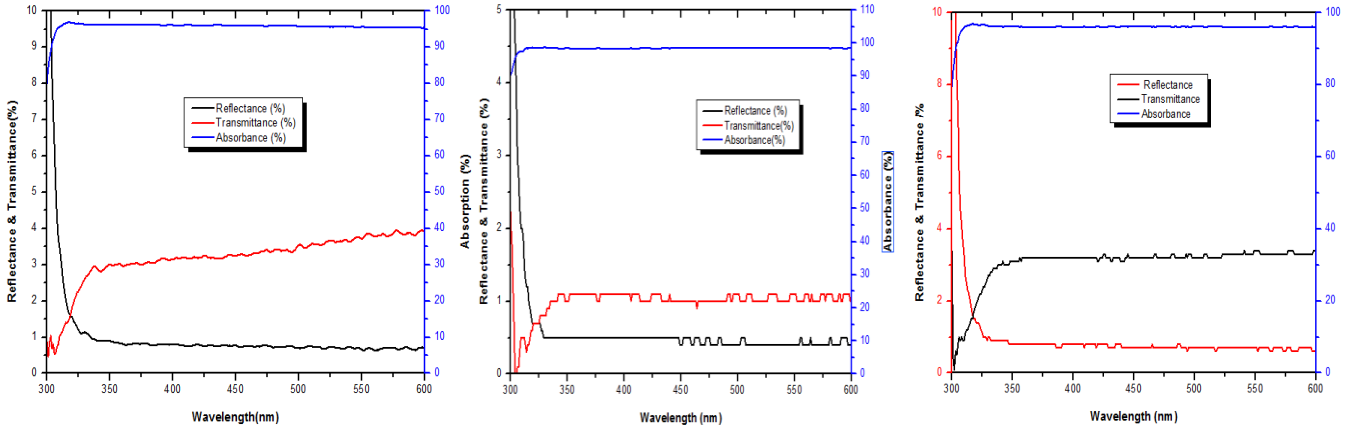

Sample 1 Sample 2 Sample 3

Fig. 2. The change of absorbance, transmittance and reflectance of CZTS films with wavelengths of three sample 1,2 & 3 at dip coating speed 100, 75 & 50ms^{-1}subsequently.

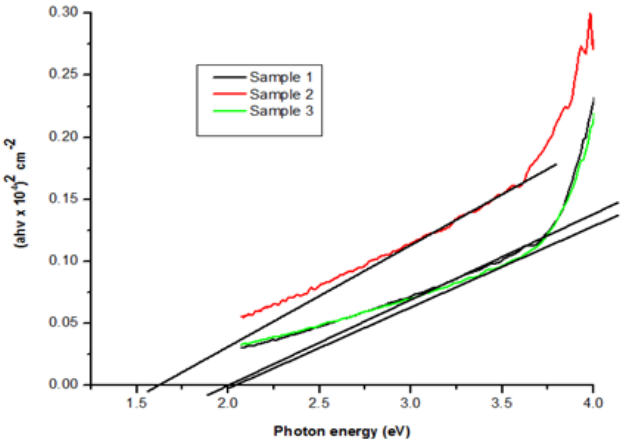

Fig. 3. Tauc plot of the CZTS thin films

3.3. Structural studies

The vacuum annealing of CZTS films at 550°C for half an hour improved the crystallinity of the CZTS thin films. Without annealing the deposited CZTS film showed no diffraction peaks. For structural studies only sample 2 (dip coating speed, 75ms^{-1}) was chosen since it gave the highest absorbance (98.3%) and optimum bang gap (close to 1.5eV). Fig. 4 shows the XRD patterns of the vacuum annealed CZTS thin films onto glass substrate. It is shown in Figure 4, that the CZTS films have the major characteristics diffraction peaks at angles 2θ= 28.4°, 31.84°, 32.898°, 47.25° and 56.10° along the (112), (103), (200), (220) and (312) planes respectively. The XRD spectra revealed that the CZTS crystal are polycrystalline nature with kesterite tetragonal crystal structure [37] [JCPDS card no. 26–0575]. From the XRD spectral information the lattice parameters "a" and "c" of the CZTS thin films were calculated. The average lattice parameter "a" of the CZTS thin films were attained as a= 0.5421nm. The obtained value of the lattice parameter "a" was very close to the standard value of the lattice parameter "a_o= 0.5435nm" of the CZTS crystal. The lattice parameter "c" of the CZTS kesterite crystal was determined and the average lattice parameter "c" for the CZTS thin films were attained as c= 1.067nm. The obtained value of the lattice parameters "c" was very close to the standard value of the lattice parameter "c_o= 1.0843nm" of the CZTS crystal. The average grain size "D" of the CZTS thin films was obtained as 23.62nm. The calculated lattice parameters and grain size values for each type of sample are shown in Table 1.

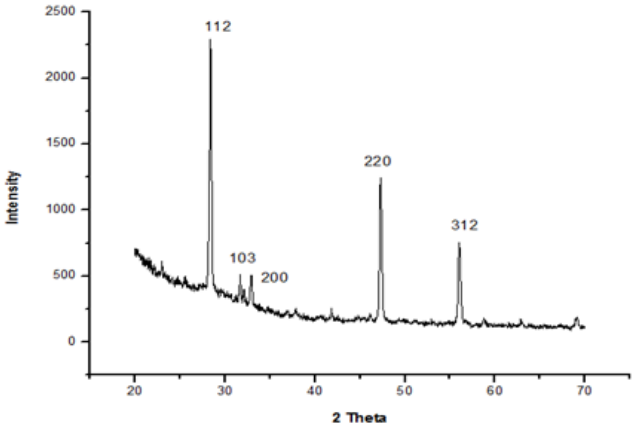

Fig. 4. The XRD patterns of the vacuum annealed CZTS thin filmsof sample 2.

3.4. Surface morphology and compositional studies

For surface morphology and compositional studies, also the sample 2 was considered for having the highest absorbance and optimum band gap. Fig. 5 (a & b) displays scanning electron micrographs of the deposited CZTS thin films at 20,000X and 500X magnifications. It is observed from the SEM images that the CZTS thin films have compact, dense in nature and non-uniform distribution of agglomerated particles with well-defined boundaries. The CZTS films are covered with rough surface. Large agglomeration of grains is noticed, which is favourable for photovoltaic utilizations, as it will reduce the recombination rate of the photo-generated electron [51, 52].

Identical kind of homogeneous, polycrystalline and extremely dense CZTS thin film was achieved by Caballero et al. [53]. Riha et al. [54] made heavily packed nano crystals, which are dispersed uniformly all over the whole surface of the substrate free from cracks or voids. Pawar et al. [50] noticed dense and orderly flat grains for the CZTS film made by electrode position technique in existence of complexing agent. Wangperawong et al. [47]demonstrated analogous dense packed morphology for Cu_2ZnSnS_4 from the aqueous bath method.

The elemental investigation of the annealed CZTS thin film was accomplished by EDS method(Fig. 6). The deposited CZTS thin films showed atomic weight percentage ratios for Cu: Zn: Sn: S as 1.9**:**1.35**:**1**:**5.2.

Hence, this type of thin film was poor in copper but rich in zinc and sulphur (exact stoichiometric ratio - Cu: Zn: Sn: S= 2**:**1**:**1**:**4) and this composition is widely found in the literature for high efficiency solar cell[24, 28, 40].

Table 1. The lattice parameters of the deposited CZTS thin films of sample 2

d /nm	hkl	2θ /°	a /nm	Average a /nm	C /nm	Average c/nm	Standard a_o/nm	Standard c_o/nm	β/°	D /nm	Average D /nm
0.3157	112	28.25	0.542		1.1139				0.294	29.17	
0.2835	103	31.545	0.5422		0.9977				0.5961	16.78	
0.271	200	32.99	0.542	0.5421		1.067	0.5435	1.0843	0.921	12.39	23.62
0.1919	220	47.41	0.5422						0.2856	31.73	
0.1635	312	56.125	0.542		1.0857				0.3358	28.04	

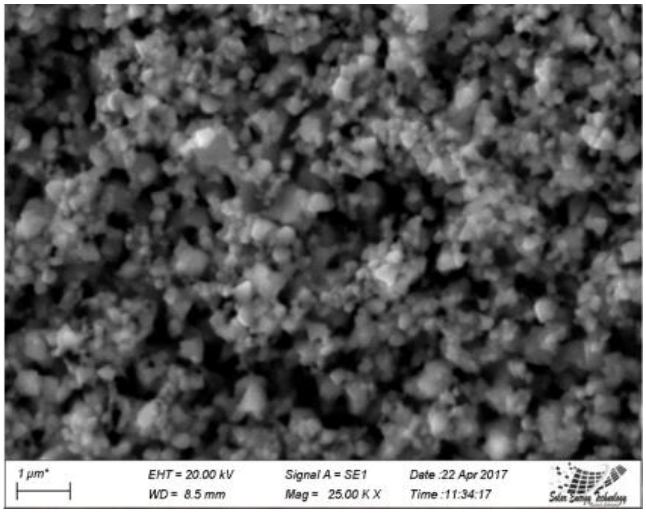

(a)

(b)

Fig. 5. The surface morphology of the CZTS thin films (a) SEM image at magnification 20000X (b) SEM image at magnification 500X of sample 2.

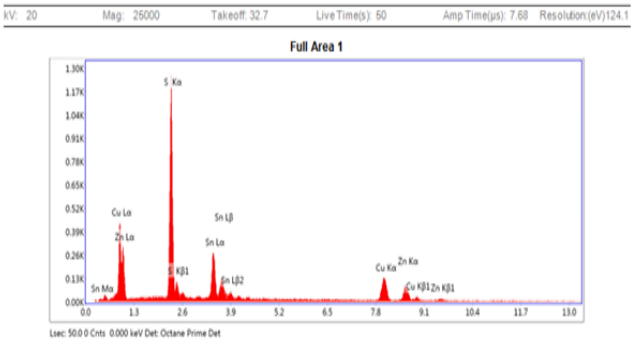

eZAF Smart Quant Results

Element	Weight %	Atomic %	Net Int.	Error %	Kratio	Z	R	A	F
S K	33.3	64.6	202.8	5.2	0.2674	1.1484	0.9238	0.6905	1.0115
SnL	24.0	10.6	64.0	8.3	0.1946	0.8465	1.1295	0.9328	1.0253
CuK	24.7	20.4	39.9	6.8	0.2510	0.9682	1.0058	0.9734	1.0787
ZnK	17.9	14.4	23.9	10.0	0.1819	0.9680	1.0096	0.9778	1.0708

Fig. 6. The EDS image and the compositional elemental analysis of the CZTS thin films of sample 2.

4. Conclusions

In this paper, a solution-based technique for the fabrication of effective CZTS thin film absorber layer solar cells has been addressed. So as to understand how carriers are generated and moved in the absorber layer, the optical and structural properties of CZTS films were studied. The characterization outcome proposed that it is rather an easy, practical and inexpensive technique for manufacturing the CZTS films. The overall device fabrication techniques are readily scalable and can easily be adapted to flexible or rigid substrates.

References

1. M. C. I. Repins, M. Romero, Y. Yan, W. Metzger, J. Li, S. Johnston, B. Egaas, C. DeHart, and J. Scharf, B.E. McCandless, R. Noufi "Characterization of 19.9%-Efficient CIGS Absorbers" *The 33rd IEEE Photovoltaic Specialists Conference,* vol. NREL/CP-520-42539, 2008.
2. D. B. Mitzi, "Solution Processing of Chalcogenide Semiconductors via Dimensional Reduction," *Advanced Materials,* vol. 21, no. 31, pp. 3141-3158, 2009.
3. M. Y. David, B. Mitzi, W. Liu, A. J. Kellock, S. J. Chey, Vaughn Deline, Alex G Schrott, "A High-Efficiency Solution-Deposited Thin-Film Photovoltaic Device," *Advanced Materials,* vol. 20, no. 19, pp. 3657-3662, 2008.
4. J. Britt, and C. Ferekides, "Thin-film CdS/CdTe solar cell with 15.8% efficiency," *Applied Physics Letters,* vol. 62, no. 22, pp. 2851-2852, 1993.
5. M. Green, K. Emery, Y. Hishikawa, W. Warta, and E. Dunlop, *Solar cell efficiency tables (version 48): Solar cell efficiency tables (version 48),* 2016.
6. Q. Guo, H. W. Hillhouse, and R. Agrawal, "Synthesis of Cu_2ZnSnS_4 nanocrystal ink and its use for solar cells," *J Am Chem Soc,* vol. 131, no. 33, pp. 11672-3, 2009.
7. C. Steinhagen, M. G. Panthani, V. Akhavan, B. Goodfellow, B. Koo, and B. A. Korgel, "Synthesis of Cu(2)ZnSnS(4) nanocrystals for use in low-cost photovoltaics," *J Am Chem Soc,* vol. 131, no. 35, pp. 12554-5, 2009.
8. B. L. Guo, Y. H. Chen, X. J. Liu, W. C. Liu, and A. D. Li, "Optical and electrical properties study of sol-gel derived Cu_2ZnSnS_4 thin films for solar cells," *AIP Advances,* vol. 4, no. 9, pp. 097115, 2014.
9. J. He, L. Sun, N. Ding, H. Kong, S. Zuo, S. Chen, Y. Chen, P. Yang, and J. Chu, "Single-step preparation and characterization of $Cu_2ZnSn(S(x)Se(1-x)_4$ thin films deposited by pulsed laser deposition method," *Journal of Alloys and Compounds,* vol. 529, no. Supplement C, pp. 34-37, 2012.
10. C. Shi, G. Shi, Z. Chen, P. Yang, and M. Yao, "Deposition of Cu_2ZnSnS_4 thin films by vacuum thermal evaporation from single quaternary compound source," *Materials Letters,* vol. 73, no. Supplement C, pp. 89-91, 2012.
11. T. Washio, T. Shinji, S. Tajima, T. Fukano, T. Motohiro, K. Jimbo, and H. Katagiri, "6% Efficiency Cu2ZnSnS4-based thin film solar cells using oxide precursors by open atmosphere type CVD," *Journal of Materials Chemistry,* vol. 22, no. 9, pp. 4021-4024, 2012.

12. M. Banavoth, S. Dias, and S. B. Krupanidhi, "Near-infrared photoactive Cu_2ZnSnS_4 thin films by co-sputtering," *AIP Advances,* vol. 3, no. 8, pp. 082132, 2013.

13. K. Tanaka, Y. Fukui, N. Moritake, and H. Uchiki, "Chemical composition dependence of morphological and optical properties of Cu_2ZnSnS_4 thin films deposited by sol–gel sulfurization and Cu_2ZnSnS_4 thin film solar cell efficiency," *Solar Energy Materials and Solar Cells,* vol. 95, no. 3, pp. 838-842, 2011.

14. Y. Wang, Y. Huang, A. Y. S. Lee, C. F. Wang, and H. Gong, "Influence of sintering temperature on screen printed Cu_2ZnSnS_4 (CZTS) films," *Journal of Alloys and Compounds,* vol. 539, no. Supplement C, pp. 237-241, 2012.

15. Z. Yan, A. Wei, Y. Zhao, J. Liu, and X. Chen, "Growth of Cu_2ZnSnS_4 thin films on transparent conducting glass substrates by the solvothermal method," *Materials Letters,* vol. 111, no. Supplement C, pp. 120-122, 2013.

16. T. K. Todorov, J. Tang, S. Bag, O. Gunawan, T. Gokmen, Y. Zhu, and D. B. Mitzi, "Beyond 11% Efficiency: Characteristics of State-of-the-Art $Cu_2ZnSn(S,Se)_4$ Solar Cells," *Advanced Energy Materials,* vol. 3, no. 1, pp. 34-38, 2013.

17. W. M. Wang W, Gunawan O, Gokmen T,Todorov TK, Zhu Y, Mitzi DB. , " Device characteristics of CZTSSe thin-film solar cells with 12.6% efficiency.," *Advanced Energy Materials* vol. 4, no. 7, 2013.

18. P. Jackson, D. Hariskos, R. Wuerz, O. Kiowski, A. Bauer, T. Magorian Friedlmeier, and M. Powalla, *Cover Picture: Properties of Cu(In,Ga)Se_2 solar cells with new record efficiencies up to 21.7% (Phys. Status Solidi RRL 1/2015),* 2015.

19. G. Y. Kim, D.-H. Son, T. T. T. Nguyen, S. Yoon, M. Kwon, C.-W. Jeon, D.-H. Kim, J.-K. Kang, and W. Jo, "Enhancement of photo-conversion efficiency in $Cu_2ZnSn(S,Se)_4$ thin-film solar cells by control of ZnS precursor-layer thickness," *Progress in Photovoltaics: Research and Applications,* vol. 24, no. 3, pp. 292-306, 2016.

20. G. O. Mitzi, D. B. Todorov, T. K. K. Wang, S. Guha, "The path towards a high-performance solution processed kesterite solar cell.," *Solar Energy Materials and Solar Cell,* vol. 95, pp. 1421–1436, 2011.

21. B. Shin, O. Gunawan, Y. Zhu, N. A. Bojarczuk, S. J. Chey, and S. Guha, "Thin film solar cell with 8.4% power conversion efficiency using an earth-abundant Cu_2ZnSnS_4 absorber," *Progress in Photovoltaics: Research and Applications,* vol. 21, no. 1, pp. 72-76, 2013.

22. A. Walsh, S. Chen, S.-H. Wei, and X.-G. Gong, "Kesterite Thin-Film Solar Cells: Advances in Materials Modelling of Cu_2ZnSnS_4," *Advanced Energy Materials,* vol. 2, no. 4, pp. 400-409, 2012.

23. T. Tanaka, D. Kawasaki, M. Nishio, Q. Guo, and H. Ogawa, "Fabrication of Cu_2ZnSnS_4 thin films by co-evaporation," *physica status solidi (c),* vol. 3, no. 8, pp. 2844-2847, 2006.

24. H. Katagiri, K. Jimbo, W. S. Maw, K. Oishi, M. Yamazaki, H. Araki, and A. Takeuchi, "Development of CZTS-based thin film solar cells," *Thin Solid Films,* vol. 517, no. 7, pp. 2455-2460, 2009.

25. K. Hironori, J. Kazuo, Y. Satoru, K. Tsuyoshi, M. Win Shwe, F. Tatsuo, I. Tadashi, and M. Tomoyoshi, "Enhanced Conversion Efficiencies of Cu_2 $ZnSnS_4$ -Based Thin Film Solar Cells by Using Preferential Etching Technique," *Applied Physics Express,* vol. 1, no. 4, pp. 041201, 2008.

26. K. Jimbo, R. Kimura, T. Kamimura, S. Yamada, W. S. Maw, H. Araki, K. Oishi, and H. Katagiri, "Cu_2ZnSnS_4-type thin film solar cells using abundant materials," *Thin Solid Films,* vol. 515, no. 15, pp. 5997-5999, 2007/05/31/, 2007.

27. A. Polizzotti, I. L. Repins, R. Noufi, S.-H. Wei, and D. B. Mitzi, "The state and future prospects of kesterite photovoltaics," *Energy & Environmental Science,* vol. 6, no. 11, pp. 3171-3182, 2013.

28. W.-C. Hsu, I. Repins, C. Beall, C. DeHart, B. To, W. Yang, Y. Yang, and R. Noufi, "Growth mechanisms of co-evaporated kesterite: a comparison of Cu-rich and Zn-rich composition paths," *Progress in Photovoltaics: Research and Applications,* vol. 22, no. 1, pp. 35-43, 2014.

29. S. Chen, A. Walsh, J.-H. Yang, X. G. Gong, L. Sun, P.-X. Yang, J.-H. Chu, and S.-H. Wei, "Compositional dependence of structural and electronic properties of Cu${}_{2}$ZnSn(S,Se)${}_{4}$ alloys for thin film solar cells," *Physical Review B,* vol. 83, no. 12, pp. 125201, 2011.

30. A. Fairbrother, E. Garcia-Hemme, V. Izquierdo-Roca, X. Fontane, F. A. Pulgarin-Agudelo, O. Vigil-Galan, A. Perez-Rodriguez, and E. Saucedo, "Development of a selective chemical etch to improve the conversion efficiency of Zn-rich Cu_2ZnSnS_4 solar cells," *J Am Chem Soc,* vol. 134, no. 19, pp. 8018-21, 2012.

31. C. Platzer-Björkman, J. Scragg, H. Flammersberger, T. Kubart, and M. Edoff, "Influence of precursor sulfur content on film formation and compositional changes in Cu_2ZnSnS_4 films and solar cells," *Solar Energy Materials and Solar Cells,* vol. 98, no. Supplement C, pp. 110-117, 2012.

32. Z. Guan, W. Luo, and Z. Zou, "Formation mechanism of ZnS impurities and their effect on photoelectrochemical properties on a Cu_2ZnSnS_4 photocathode", 2014.

33. D. Seo, and S. Lim, "Effect of sulfur and copper amounts in sol–gel precursor solution on the growth, crystal properties, and optical properties of Cu_2ZnSnS_4 films", 2013.

34. H. Katagiri, K. Saitoh, T. Washio, H. Shinohara, T. Kurumadani, and S. Miyajima, "Development of thin film solar cell based on Cu_2ZnSnS_4 thin films," *Solar Energy Materials and Solar Cells,* vol. 65, no. 1, pp. 141-148, 2001.

35. D. Ginley, M. A. Green, and R. Collins, "Solar Energy Conversion Toward 1 Terawatt," *MRS Bulletin,* vol. 33, no. 4, pp. 355-364, 2008.

36. T. Tanaka, T. Nagatomo, D. Kawasaki, M. Nishio, Q. Guo, A. Wakahara, A. Yoshida, and H. Ogawa, "Preparation of Cu_2ZnSnS_4 thin films by hybrid sputtering," *Journal of Physics and Chemistry of Solids,* vol. 66, no. 11, pp. 1978-1981, 2005.

37. K. Tanaka, M. Oonuki, N. Moritake, and H. Uchiki, "Cu_2ZnSnS_4 thin film solar cells prepared by non-vacuum processing," *Solar Energy Materials and Solar Cells,* vol. 93, no. 5, pp. 583-587, 2009.

38. I. Kentaro, and N. Tatsuo, "Electrical and Optical Properties of Stannite-Type Quaternary Semiconductor Thin Films," *Japanese Journal of Applied Physics,* vol. 27, no. 11R, pp. 2094, 1988.

39. J.-S. Seol, S.-Y. Lee, J.-C. Lee, H.-D. Nam, and K.-H. Kim, "Electrical and optical properties of Cu_2ZnSnS_4 thin films prepared by rf magnetron sputtering process," *Solar Energy Materials and Solar Cells,* vol. 75, no. 1, pp. 155-162, 2003.

40. T. K. Todorov, K. B. Reuter, and D. B. Mitzi, "High-efficiency solar cell with Earth-abundant liquid-processed absorber," *Adv Mater,* vol. 22, no. 20, pp. 200904155, 2010.

41. J. J. Scragg, P. J. Dale, L. M. Peter, G. Zoppi, and I. Forbes, "New routes to sustainable photovoltaics: evaluation of Cu_2ZnSnS_4 as an alternative absorber material," *Physica Status Solidi (b),* vol. 245, no. 9, pp. 1772-1778, 2008.

42. A. Fischereder, T. Rath, W. Haas, H. Amenitsch, J. r. Albering, D. Meischler, S. Larissegger, M. Edler, R. Saf, and F. Hofer, "Investigation of Cu_2ZnSnS_4 formation from metal salts and thioacetamide," *Chemistry of Materials,* vol. 22, no. 11, pp. 3399-3406, 2010.

43. S. M. Pawar, B. S. Pawar, A. V. Moholkar, D. S. Choi, J. H. Yun, J. H. Moon, S. S. Kolekar, and J. H. Kim, "Single step electrosynthesis of Cu_2ZnSnS_4 (CZTS) thin films for solar cell application," *Electrochimica Acta,* vol. 55, no. 12, pp. 4057-4061, 2010.

44. H. M. Pathan, and C. D. Lokhande, "Deposition of metal chalcogenide thin films by successive ionic layer adsorption and reaction (SILAR) method," *Bull. of Mater. Sci.,* vol. 27, no. 2, pp. 85-111, April 01, 2004.

45. J. A. Thornton, "The microstructure of sputter-deposited coatings," *Journal of Vacuum Science & Technology A,* vol. 4, no. 6, 1986.

46. K. Tanaka, N. Moritake, and H. Uchiki, "Preparation of Cu_2ZnSnS_4 thin films by sulfurizing sol–gel deposited precursors," *Solar Energy Materials and Solar Cells,* vol. 91, no. 13, pp. 1199-1201, 2007.

47. A. Wangperawong, J. S. King, S. M. Herron, B. P. Tran, K. Pangan-Okimoto, and S. F. Bent, "Aqueous bath process for deposition of $Cu_2ZnSnS4$ photovoltaic absorbers," *Thin Solid Films,* vol. 519, no. 8, pp. 2488-2492, 2011.

48. I. Kriegel, J. Rodríguez-Fernández, E. D. Como, A. A. Lutich, J. M. Szeifert, and J. Feldmann, "Tuning the Light Absorption of Cu1.97S Nanocrystals in Supercrystal Structures," *Chemistry of Materials,* vol. 23, no. 7, pp. 1830-1834, 2011.

49. J. M. Luther, P. K. Jain, T. Ewers, and A. P. Alivisatos, "Localized surface plasmon resonances arising from free carriers in doped quantum dots," *Nat Mater,* vol. 10, no. 5, pp. 361-6, 2011.

50. B. S. Pawar, S. M. Pawar, S. W. Shin, D. S. Choi, C. J. Park, S. S. Kolekar and J. H. Kim, "Effect of complexing agent on the properties of electrochemically deposited Cu_2ZnSnS_4 (CZTS) thin films," *Applied Surface Science,* vol. 257, no. 5, pp. 1786-1791, 2010.

51. Y. Zhao, H. Pan, Y. Lou, X. Qiu, J. Zhu, and C. Burda, "Plasmonic $Cu_{(2-x)}S$ nanocrystals: optical and structural properties of copper-deficient copper(I) sulfides," *J Am Chem Soc,* vol. 131, no. 12, pp. 4253-61, 2009.

52. G. M. Ford, Q. Guo, R. Agrawal, and H. W. Hillhouse, "Earth Abundant Element $Cu_2Zn(Sn_{1-x}Ge_x)S_4$ Nanocrystals for Tunable Band Gap Solar Cells: 6.8% Efficient Device Fabrication," *Chemistry of Materials,* vol. 23, no. 10, pp. 2626-2629, 2011.

53. R. Caballero, C. Maffiotte, and C. Guillén, "Preparation and characterization of $CuIn_{1-x}Ga_xSe_2$ thin films obtained by sequential evaporations and different selenization processes," *Thin Solid Films,* vol. 474, no. 1, pp. 70-76, 2005.

54. S. C. Riha, S. J. Fredrick, J. B. Sambur, Y. Liu, A. L. Prieto, and B. A. Parkinson, "Photoelectrochemical characterization of nanocrystalline thin-film Cu(2)ZnSnS(4) photocathodes," *ACS Appl Mater Interfaces,* vol. 3, no. 1, pp. 58-66, 2011.